LOGIC
Journal of Engineering Design and Technology
Vol. 24 No.2 July 2024 ; p. 39-48

p-ISSN : 1412-114X
e-ISSN : 2580-5649
http://ojs2.pnb.ac.id/index.php/LOGIC

EFFECT OF STATIC THERMAL TENSIONING AND PREHEATING ON ANGULAR DISTORTION IN FCAW WELDED SS400 STEEL CORNER JOINTS

Sugeng Hadi Susilo [1)*], Eko Yudiyanto[2)], Agus Setiawan[3)], Khambali[4)], Suyanto[5)], Falih Alauddin[6)]

[1,2,3,4,5,6)] Department of Mechanical Engineering, Politeknik Negeri Malang, Jalan Soekarno-Hatta No 9, Jatimulyo, Lowokwaru, Malang, Indonesia

Correponding email [1)*] : Sugeng.hadi@polinema.ac.id

Abstract.
FCAW welding is an automated welding process that uses wire-wound electrodes to melt metal, using flux or powder inside the electrode core for protection. Common problems in FCAW welding are angular distortion and changes in length and width dimensions, especially in thin plate iron materials, due to residual stress from the welding process.
This research aims to examine the impact of static thermal stress, preheating, and their combination on corner distortion in SS400 steel corner joints during FCAW welding, taking into account the heat input during welding. An actual experimental research methodology was used, with varying preheating temperatures of 200°C, 250°C, 300°C, static thermal stress at 150°C, 200°C, 250°C, transient thermal stress at 150°C, 200° C, 250 °C, and an untreated reference method to determine the welding approach that minimizes corner distortion. The material used is 3mm thick SS400 steel.
The research results show that there is a significant influence of static thermal stress, preheating, and a combination of both on corner distortion. The optimal welding methods identified are preheating static thermal stress at 89°55', preheating transient thermal stress at 89°50', static thermal stress at 150°C at 89°45', transient thermal stress at 150°C at 89 '. °40', and preheating at 200°C at 89°35'.

Keywords : Angular Distortion, SS400 Steel, FCAW Welding

1. INTRODUCTION

Manufacturing requires welding to combine parts and construct structures. Metals can be joined locally with arc welding's high heat. Conduction cools a base metal after moving a molten wire to it in the consumable electrode method. Shrinkage owing to heat strain induces partial transition into tensile plastic strain in unbounded areas. This causes persistent deformation in the base material because compressive plastic strain during heating exceeds tensile strain during cooling. Uneven shrinkage and greater lattice spacing leave residual tensile stresses. Compressive stress remains in the surrounding environment [1]. Residual tensile stress affects fatigue life, stress corrosion cracking, weld cracking, and bending strength [2].
Welding distortions cause geometric misalignments and gaps between structures, which complicate assembly and reduce manufacturing quality and productivity. Due to their thickness, offshore platform and ship hull legs, nodes, major frames, and girders are multi-layer welded to handle enormous stresses. As a geometric flaw, welding's initial distortion might impair bending strength under compressive force. We know initial deflection reduces bending strength. Similar to the shear line formula with eccentric loading, the initial curvature in the deflection affects bending strength [3]. Welding distortion prediction and control are crucial.
Based on this notion, DNV GL standards [4] set structural design alignment and straightness tolerances. Product

design and manufacturing in shipbuilding and heavy industries follow these guidelines to prevent buckling tragedies. In additive manufacturing (AM), multi-layer deposition has caused thermal deformation concerns as well as conventional industries. In AM parts, thermal deformation produces dimensional inaccuracies, and prediction equations developed from measured strain data advise changing laser power, layer thickness, and scanning speed to reduce thermal strain [5].

Clamping force matters most in thermal deformation, which is affected by material qualities, temperature, and cross-sectional area [6]. With layer deposition, displacement increased proportionately. Uneven thickness-direction transverse shrinkage distorts the welding angle in one pass [7]. This distortion depends on weld deposition, thickness temperature gradient, and limitations. The direction and amount of the angular distortion depend on the bead cross-sectional profile asymmetry, according to laser welding studies and theoretical models [8]. Cross-sectional bead deposition vary with methods and circumstances. Weld material, plastic strain distribution, and holes also affect angular distortion. Fluid flow deposited at groove joints, radiation, and convection cooling conditions, and material thermal characteristics determine temperature dispersion.

Temperature gradients dominate corner distortion in fillet welding simulations [9]. According to [10], the beginning temperature affects the thickness temperature gradient by angular distortion. Pre- and post-heating treatments affected temperature distribution, residual strains, and distortion [11]. Due to high-temperature stiffness loss, early setup and installation conditions dictate distortion. Many foundational studies have examined welding distortion in different situations and materials.

When penetration is less than 0.6 times thickness, [12] discovered that the angular distortion of bead-on-plate welding is linearly linked to heat input (H) to the square of thickness (t). As penetration rises, the non-fusion zone below the fusion zone becomes plastic owing to temperature increase and is difficult to use as a rotation point for bending.

Numerous tests examined how heat input, plate thickness, and materials affect deformation [13]. This formula predicts welding distortion using heat flow and thermal elastoplast theory. According to studies, welding distortion in the same material depends on H/t^2 (heat input divided by thickness squared). Regardless of the welding technique, mild steel distortion is proportionate to H/t^2 when H/t^2 is less than 2500 cal/cm^3.

Thermal elastoplasts' intrinsic strain mechanism was used to create an elastic model [14]. Their database shows that transverse angular distortion rises until H/t^2 reaches 10 kJ/mm^3 and then falls to 40. Deformation depends on heat and thickness. Angular distortion increases with heat input and decreases with thickness squared after a maximum. Since molten wire fills the groove between the plates, the number of passes depends on the metal deposit per length. The physics of arc welding has also been used to study wire melting.

Calculations determined SAW bead dimensions [15]. Travel speed and nozzle-to-plate distance decreased bead area, whereas wire feed rate and arc voltage increased HAZ. Wire feed rate increases bead size, whereas arc voltage widens but reduces penetration and gain. Weld bead size prediction methodology for 409 M stainless steel gas metal arc welding (GMAW) employing central composite rotating design [16]. During welding, current increased penetration, width, reinforcement, and thinning, while speed decreased bead dimensions and arc voltage increased all but reinforcement. SAW matches FCAW. Explored welding variables and bead shape/HAZ width [17]. Speed reduces weld metal cross-sectional area and HAZ width.

Response surface regression was used to estimate FCAW 317L cladding weld form [18]. Our welding current increases penetration, bead size, and area. Electric current dominates bead size because resistance melts electrode wire [19, 20]. Bead form and welding process factors affected fatigue life [21]. The bead aspect ratio between maximum height and joint width fluctuates with heat input, impacting fatigue life.

2. METHODS

Using SS 400 steel with a thickness of 3 mm. The welding machine used is an OTC brand FCAW welding machine, Japanese inventor model, with a current setting of 120 A, voltage 25 volts, straight polarity, AWS E71T1 electrode with a diameter of 1.2 mm, flat position and corner joint welding type.

2.1 Welding Process

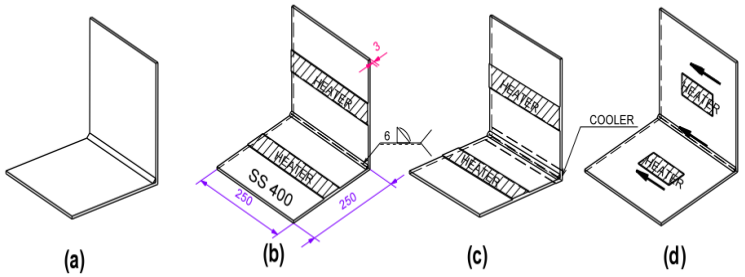

Figure 1 Welding Method

Description
(a) Without treatment
(b) Preheating
(c) Static Thermal Tensioning
(d) Transient Thermal Tensioning

2.1.1 Welding Process Without Treatment

This welding process aims to determine the initial results of distortion data whether later after the welding process with various methods can minimize the occurrence of distortion or increase the amount of distortion. Welding is done without additional heating in the base metal.

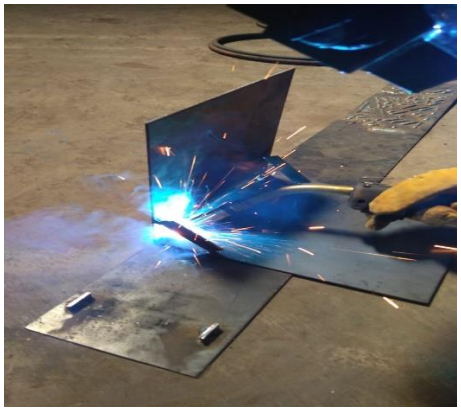

Figure 2 Welding process without treatment

The results of distortion measurements using a universal bevel protractor can be seen in Figure 3.

Figure 3 Distortion measurement results of the welding method without treatment

2.1.2 Preheating Process

Welding with preheating is carried out before the welding process, the heating is directed evenly in the base metal to be welded with the aim of minimizing angular distortion with heating temperature variations of 200°, 250° and 300°. Heating is done with an additional heating device in the form of oxy gas. The measurement results with the universal bevel protractor are as shown in Figure 4.

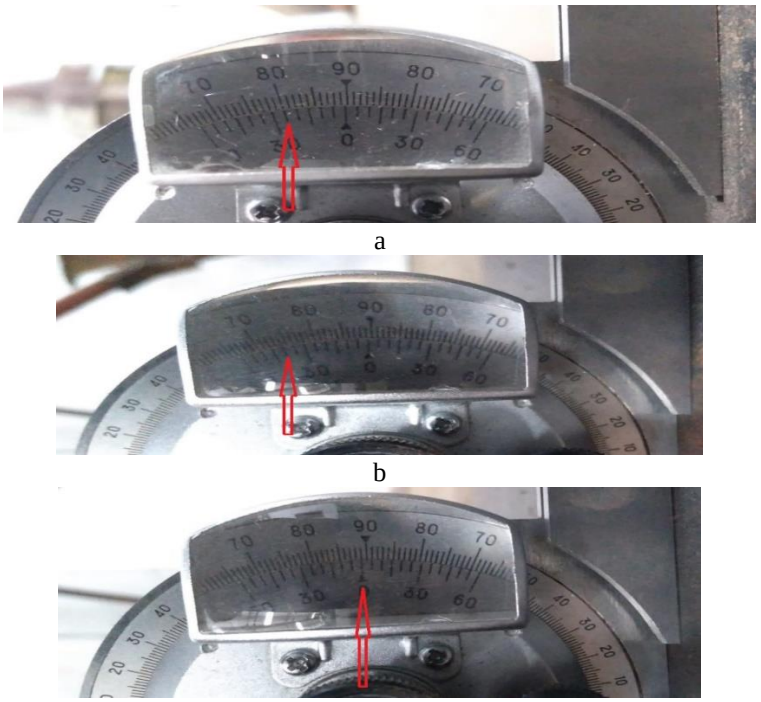

a

b

c

Figure 4 Measurement results using the preheating process: a. Temperature 200°C, b. Temperature 250°C, c. Temperature 300°C.

2.1.3 Static Thermal Tensioning Process

Welding with static thermal tensioning is carried out during the welding process with heat output and also a cooler. Heating is carried out with oxy gas and cooling with water during welding with heating temperature variations of 150°, 200° and 250°. The results of welding gauge measurements on the static thermal tensioning process are as shown in Figure 5.

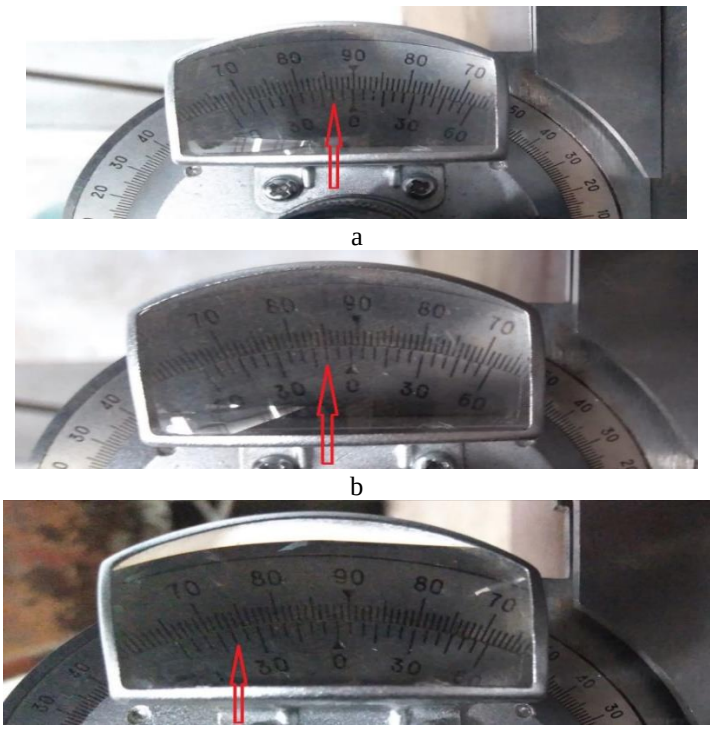

a

b

c

Figure 5 Results of static thermal tensioning distortion measurements: a. temperature 150°C, b. temperature 200°C, c. temperature 250°C.

2.1.4 Transient Thermal Tensioning Process

Welding using a transient thermal tensioning process is carried out during the welding process with a heat output and cooler. Heating is carried out with oxy gas and is directed behind the welding arc and cooler together, with heating temperature variations of 150°, 200°, 250°. The results of welding gauge measurements in the transient thermal tensioning process are as shown in Figure 6.

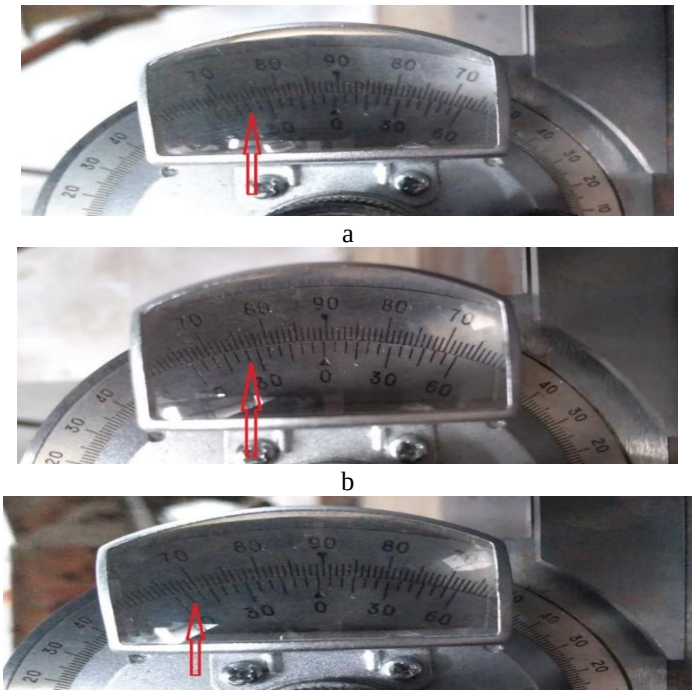

a b c

Figure 6 Distortion results of the transient thermal tensioning process: a. temperature 150°C, b. temperature 200°C, c. Temperature 250°C.

2.1.5 Preheating-Static Thermal Tensioning Process

Welding with this process is carried out through two heat treatments, heating the base metal before welding (preheating) and heating the base metal during the welding process with constant heat with a preheat heating temperature of 200°C and static thermal tensioning 150°C. The results of distortion measurements using a welding gauge in the preheating-static thermal tensioning process are as shown in Figure 7.

Figure 7 Results of measuring distortion data for the preheating-Static thermal tensioning process

2.1.6 Preheating-Transient Thermal Tensioning Process

Welding with this process is carried out two heat treatments, heating the base metal before welding (preheating) and heating the base metal during the welding process, the position of the heater and coolant following behind the welding arc with a preheat temperature of 200°C and transient thermal tensioning of 150°C .
The results of distortion measurements using a welding gauge are as shown in Figure 8.

Figure 8 Results of measuring distortion data from the preheating-transient thermal tensioning process

3. RESULTS AND DISCUSSION

3.1 Results

The data obtained in this research comes from the results of distortion measurements with a bavel universal protractor. So that the results of the welding method are obtained to minimize distortion. The measurement results are as in Figure 9.

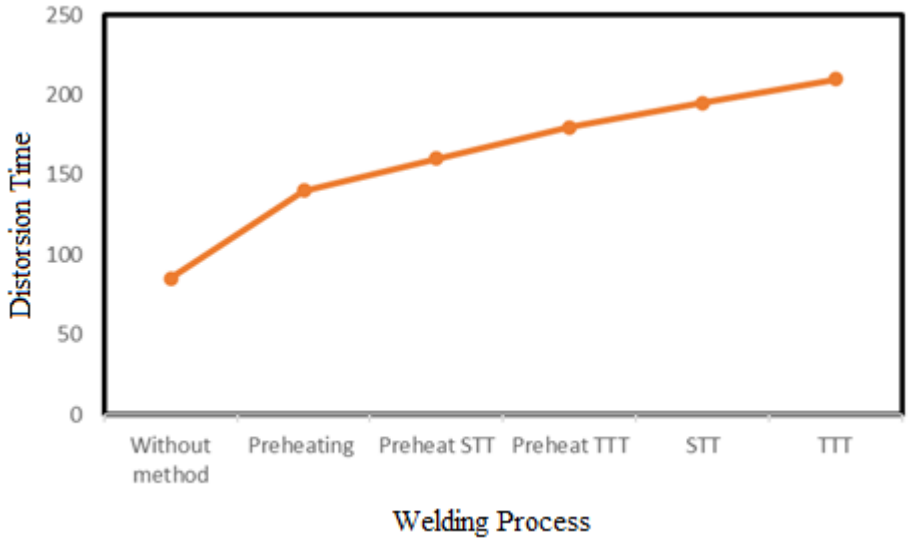

Figure 9 Welding Process

Figure 9 provides experimental data on the various welding processes used, measured in degrees. welding processes include untreated processes, preheating processes, STT preheating, TTT preheating, STT static thermal stress, and TTT transient thermal stress. The research results show the maximum temperature achieved in the welding process with each method. This temperature is an important indication of the energy level applied to the welding process and has a major influence on corner distortion in SS400 steel corner joints.

Data processing used Minitab 18 software, using the One Way Anova method, based on analysis with Minitab 18 software as shown in table 1-5.

Distortion Data versus Welding Process

Process

Null hypothesis	All means are equal
Alternative hypothesis	Not all means are equal
Significance level α	= 0.05

Table 1 Equal variances were assumed for the analysis.

Factor	Levels	Values
Welding Process	12	Preheating + STT; Preheating + TTT; Preheating 200°C; Preheating 250°C; Preheating 300°C; Static Thermal Tensioning 150°C; Static Thermal Tensioning 200°C; Static Thermal Tensioning 250°C; without threatment; Transient Thermal Tensioning 150°C; Transient Thermal Tensioning 200°C; Transient Thermal Tensioning 250°C

Table 2 Analysis of Variance Combination Preheating, Static-transient Thermal Tensioning

Source	DF	Adj SS	Adj MS	F-Value	P-Value
Welding Process	11	4,460	0,40547	9,62	0,000
Error	24	1,012	0,04215		
Total	35	5,472			

Where,

Reject H_0 if P value < 0.05

P value 0.000 < 0.05 So H_0 is rejected

This means that not all of them are the same, meaning that not all welding processes are the same or that there are significant differences between the three processes used.

Tabel 3 Analysis of Variance Preheating

Source	DF	Seq SS	Contribution	Adj SS	Adj MS	F-Value	P-Value
Welding Process	2	0,3289	68,92%	0,3289	0,16444	6,65	0,030
Error	6	0,1483	31,08%	0,1483	0,02472		
Total	8	0,4772	100,00%				

Where,
Reject H_0 if P value < 0.05
P value 0.030 < 0.05 So H_0 is rejected
This means that the preheating welding process is not the same or there are significant differences in the preheating process used.

Table 4 Analysis of Variance Static Thermal Tensioning

Source	DF	Seq SS	Contribution	Adj SS	Adj MS	F-Value	P-Value
Welding Process	2	2,0339	88,60%	2,0339	1,01694	23,32	0,001
Error	6	0,2617	11,40%	0,2617	0,04361		
Total	8	2,2956	100,00%				

Where,
Reject H_0 if P value < 0.05
P value 0.001 < 0.05 So H_0 is rejected
This means that the Static Thermal Tensioning welding process is not the same or there are significant differences in the Static Thermal Tensioning process used.

Table 5 Analysis of Variance Transient Thermal Tensioning

Source	DF	Seq SS	Contribution	Adj SS	Adj MS	F-Value	P-Value
Welding Process	2	0,4289	41,82%	0,4289	0,21444	2,16	0,197
Error	6	0,5967	58,18%	0,5967	0,09944		
Total	8	1,0256	100,00%				

Where
Reject H_0 if P value < 0.05
P value 0.197 < 0.05 So H_0 is accepted
The conclusion is that the same means the Transient Thermal Tensioning welding process or there is no significant difference in the Transient Thermal Tensioning process used. Figure 3 shows the results of measuring distortion with a universal protractor, with each re-welding process 3 times.

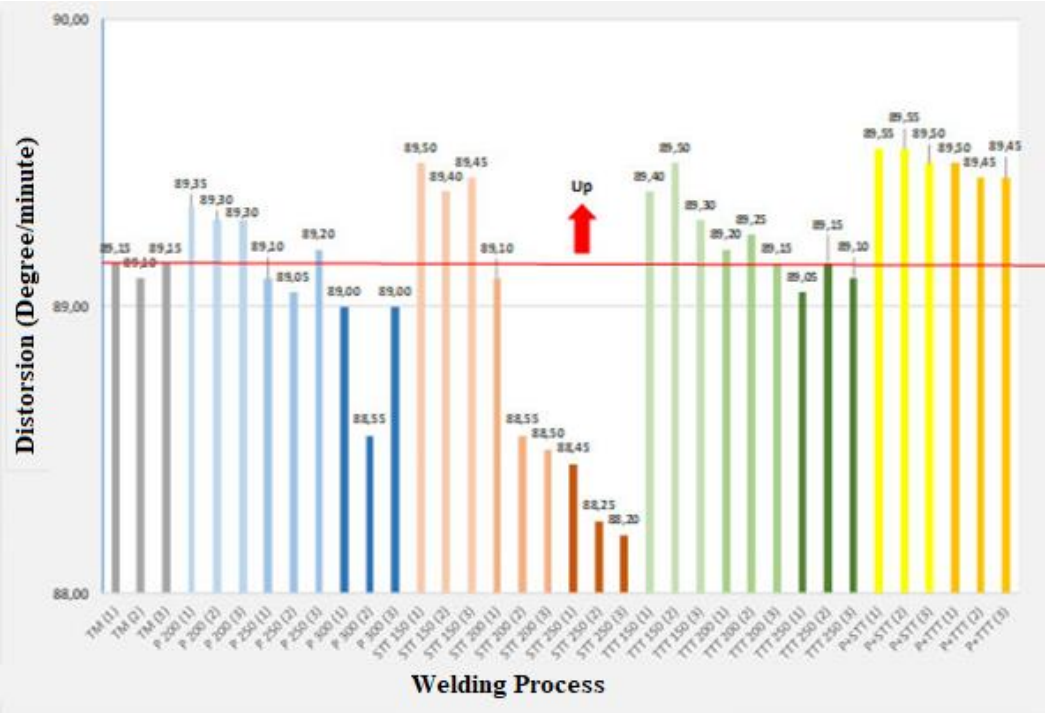

Figure 3 Distortion Data

Where,

- : Without Methods
- : Preheating 200°C
- : Preheating 250°C
- : Preheating 300°C
- : Static Thermal Tensioning 150°C
- : Static Thermal Tensioning 200°C
- : Static Thermal Tensioning 250°C
- : Transient Thermal Tensioning 150°C
- : Transient Thermal Tensioning 200°C
- : Transient Thermal Tensioning 250°C
- : Preheating + Static Thermal Tensioning
- : Preheating + Transient Thermal Tensioning

The welding process without treatment (red line) is a reference point for whether there is a change in the distortion results after several welding processes. A good welding process is above the red line. The process with good results is above the reference point, namely 89°15'. From the results of the distortion data in Figure 3, it is stated that the good results are:

• Preheating + Static Thermal Tensioning, 89°55'
• Preheating + Transient Thermal Tensioning, 89°50'
• Static Thermal Tensioning 150°C, 89°45'
• Transient Thermal Tensioning150°C, 89°40'
• Preheating 200°C, 89°35'

The results of the welding process data are no better for minimizing distortion, namely:

• Preheating 250°C, 89°10'
• Preheating 300°C, 89°
• Static Thermal Tensioning 200°C, 88°55'
• Static Thermal Tensioning 250°C, 88°25'
• Transient Thermal Tensioning250°C, 89°05'

4. CONCLUSION

The smallest distortion was obtained from a temperature variation of 150°C of 89°45', and the largest distortion was obtained with a temperature variation of 250°C of 88°20'. And there is no significant influence of the transient thermal tensioning welding method on the distortion results. The smallest distortion results were obtained from a temperature variation of 150°C of 89°40', and the largest distortion was obtained with a temperature variation of

250°C of 89°10'. Meanwhile, there is a significant influence of the preheating welding method on the distortion results. The smallest distortion results were obtained from a temperature variation of 200°C of 89°35', and the largest distortion was obtained with a temperature variation of 300°C of 89°. There is a significant influence of the combination of preheating and static-transient thermal tensioning welding methods on the distortion results. The smallest distortion result was 89°55', and the largest distortion was 89°45'.

6. REFERENCES

[1] A. Aggarwal, D. Adlakha, and P. Khanna, "Development of a mathematical model to predict angular distortion in FCA welded stainless steel 301 plates," *Mater. Today Proc.*, vol. 78, 2023, doi: 10.1016/j.matpr.2022.11.478.
[2] H. Alipooramirabad, A. Paradowska, R. Ghomashchi, and M. Reid, "Investigating the effects of welding process on residual stresses, microstructure and mechanical properties in HSLA steel welds," *J. Manuf. Process.*, vol. 28, 2017, doi: 10.1016/j.jmapro.2017.04.030.
[3] C. P. Alvarães, F. C. A. Madalena, L. F. G. De Souza, J. C. F. Jorge, L. S. Araújo, and M. C. Mendes, "Performance of the INCONEL 625 alloy weld overlay obtained by FCAW process," *Rev. Mater.*, vol. 24, no. 1, 2019, doi: 10.1590/s1517-707620190001.0627.
[4] A. V. Balan, T. Kannan, and N. Shivasankaran, "Effect of FCAW process parameters on bead geometry in super duplex stainless steel claddings," *Int. J. Appl. Eng. Res.*, vol. 9, no. 24, 2014.
[5] G. Bansal Rajkumar and N. Murugan, "Prediction of Flux cored arc welding process parameters effect on 2205 duplex stainless steel," *Weld. Cut.*, vol. 12, no. 1, 2013.
[6] A. Burgos, H. Svoboda, Z. Zhang, and E. Surian, "Alternative PWHT to Improve High-Temperature Mechanical Properties of Advanced 9Cr Steel Welds," *J. Mater. Eng. Perform.*, vol. 27, no. 12, 2018, doi: 10.1007/s11665-018-3736-5.
[7] E. Dogan, M. Ay, M. Kurtulmus, A. I. Yukler, and A. Etyemez, "Effects of welding parameters on the angular distortion of welded steel plates," *Open Chem.*, vol. 20, no. 1, 2022, doi: 10.1515/chem-2022-0152.
[8] W. A. R. Harahap, "Studi Awal Pengelasan Kombinasi GMAW-FCAW Dengan Variasi Arus Weld Metal Menggunakan Proses Wire Arc Additive Manufacturing (WAAM) Terhadap Nilai Kekuatan Tarik Dan Struktur Mikro," *Teknologi*, 2021.
[9] C. Hwang *et al.*, "Evaluation and Prediction of Formation of Heat-Affected Zone and Mechanical Properties According to Welding Method of STS 316L/A516-70N Clad Plates," *J. Korean Inst. Met. Mater.*, vol. 60, no. 12, 2022, doi: 10.3365/KJMM.2022.60.12.873.
[10] J. Jiang, J. Zhang, J. Liu, S. P. Chiew, and C. K. Lee, "Effect of welding and heat treatment on strength of high-strength steel columns," *J. Constr. Steel Res.*, vol. 151, 2018, doi: 10.1016/j.jcsr.2018.09.027.
[11] S. C. Juang and Y. S. Tarng, "Process parameter selection for optimizing the weld pool geometry in the tungsten inert gas welding of stainless steel," *J. Mater. Process. Technol.*, vol. 122, no. 1, 2002, doi: 10.1016/S0924-0136(02)00021-3.
[12] J. Kim and J. Kim, "Laser welding of astm a553-1 (9% nickel steel) (part ii: Comparison of mechanical properties with fcaw)," *Metals (Basel).*, vol. 10, no. 8, 2020, doi: 10.3390/met10080999.
[13] V. V. Kumar and N. Murugan, "Effect of FCAW Process Parameters on Weld Bead Geometry in Stainless Steel Cladding," *J. Miner. Mater. Charact. Eng.*, vol. 10, no. 09, 2011, doi: 10.4236/jmmce.2011.109064.
[14] K. H. Ling, Y. K. Fuh, T. C. Kuo, and S. Xun-Tu, "Effect of welding sequence of a multi-pass temper bead in gas-shielded flux-cored arc welding process: hardness, microstructure, and impact toughness analysis," *Int. J. Adv. Manuf. Technol.*, vol. 81, no. 5–8, 2015, doi: 10.1007/s00170-015-7277-x.
[15] M. Malhotra, Kashish, Samridhi, and P. Khanna, "Prediction of angular distortion in flux-cored arc welding of stainless steel 301 plates by mathematical modelling," *Mater. Today Proc.*, vol. 62, 2022, doi: 10.1016/j.matpr.2022.04.426.
[16] J. L. Meseguer-Valdenebro, J. Serna, A. Portoles, M. Estrems, V. Miguel, and E. Martínez-Conesa, "Experimental Validation of a Numerical Method that Predicts the Size of the Heat Affected Zone. Optimization of the Welding Parameters by the Taguchi's Method," *Trans. Indian Inst. Met.*, vol. 69, no. 3, 2016, doi: 10.1007/s12666-015-0554-4.
[17] P. K. Palani and N. Murugan, "Optimization of weld bead geometry for stainless steel claddings deposited by FCAW," *J. Mater. Process. Technol.*, vol. 190, no. 1–3, 2007, doi: 10.1016/j.jmatprotec.2007.02.035.
[18] P. K. Palani, N. Murugan, and B. Karthikeyan, "Process parameter selection for optimising weld bead geometry in stainless steel cladding using Taguchi's approach," *Mater. Sci. Technol.*, vol. 22, no. 10, 2006, doi: 10.1179/174328406X118294.
[19] M. Palpandi, G. Magudeeswaran, and N. Harikannan, "Optimization of pulsed current flux cored arc welding parameters for ferrite phase in duplex stainless steel welds," *J. Balk. Tribol. Assoc.*, vol. 26, no. 2, 2020.
[20] M. Palpandi, G. Magudeeswaran, and N. Harikannan, "Optimization of pulsed current flux cored arc

welding parameters for ferrite phase in duplex stainless steel welds," *J. Balk. Tribol. Assoc.*, vol. 25, no. 4, 2019.
[21] A. Sehrawat, "Mathematical Modelling for Prediction of Angular Distortion in MIG Welding of Stainless Steel 301," *Int. J. Res. Appl. Sci. Eng. Technol.*, vol. 8, no. 7, 2020, doi: 10.22214/ijraset.2020.30372.